archives
of thermodynamics
Vol. **42**(2021), No. 3, 279–309
DOI: 10.24425/ather.2021.138120

Refined multi-phase-lags theory and Thomson effect on a micropolar thermoelastic medium with voids

AMNAH M. ALHARBI[a]
ELSAYED M. ABD-ELAZIZ[b]
MOHAMED I.A. OTHMAN[c*]

[a] Taif University, Department of Mathematics, College of Science, P.O. Box 11099, Taif, 21944, Saudi Arabia

[b] Ministry of Higher Education, Zagazig Higher Institute of Engineering & Technology, Zagazig, Egypt

[c] Zagazig University, Department of Mathematics, Faculty of Science, P.O. Box 44519, Zagazig, Egypt

Abstract The problem considered is that of an isotropic, micropolar thermoelastic medium with voids subjected to the Thomson effect. The solution to the problem is presented in the context of the refined multi-phase-lags theory of thermoelasticity. The normal mode analysis was used to obtain the analytical expressions of the considered variables. The non-dimensional displacement, temperature, microrotation, the change in the volume fraction field and stress of the material are obtained and illustrated graphically. The variations of these quantities have been depicted graphically in the refined-phase-lag theory, Green and Naghdi theory of type II, Lord and Shulman theory and a coupled theory. The effects of the Thomson parameter and phase lag parameters on a homogeneous, isotropic, micropolar thermoelastic material with voids are revealed and discussed. Some particular cases of interest are deduced from the present investigation.

Keywords: Micropolar; Voids; Refined-phase-lags theory; Thomson effect; Normal mode analysis

*Corresponding Author. Email: m_i_a_othman@yahoo.com

Nomenclature

a – wave number in the x-direction, m
C_e – specific heat at constant strain, kJ/kgK
e – dilatation
F_0 – constant force, N/m^2
i – imaginary unit
j – microinertia,m^2
K^* – thermal conductivity, W/(m K)
k – material constants due to presence of micropolar, N/m^2
L_0 – Thomson coefficient
M – small non-dimensional constant
m_{ij} – couple stress tensor components
N – parameter, $N = 1 \ldots 7$
q_1, q_2 – displacement potentials
s – time constant, s
T – temperature above the reference temperature T_0, such that $|(T - T_0)/T_0| \ll 1$, K
T_0 – environmental temperature, K
t – time, s
$\boldsymbol{u}$ – displacement vector, $\equiv (u, v, w)$
u, v, w – displacement components, m
υ – volume thermal expansion, $= (3\lambda + 2\mu + k)\alpha_t$
x, y, z – Cartesian coordinates
∇^2 – Laplace operator
$(\dddot{\cdot})$ – number of over dots stand for the order of differentiation of a variable with respect to time

Greek symbols

α, β, γ – material constants due to presence of micropolar: (0, N/m^{2}K, N)
α_t – coefficient of linear thermal expansion, 1/K
$\alpha^*, \eta^*, \omega^*, \beta^*, m, \zeta^*$ – material constants due to presence of voids: N, N/m^2, Ns/m^2, N/m^2, N/m^{2}K, N/m^2
δ – parameter takes values either 0 or 1, according to the thermoelasticity theory applied
δ_{ij} – Kronecker delta
ε_{ij} – strain tensor components
ε_{ijr} – permutation tensor
θ – temperature increment, $= T - T_0$, K
θ_0 – constant temperature, K
λ, μ – Lamé constants, N/m^2
ρ – material density, kg/m^3
ρ_e^0 – charge density when strain vanishes, kg/m^3
σ_{ij} – stress tensor components, N/m2
τ_q – phase-lag of heat flux, s
τ_θ – phase-lag of temperature gradient, s
τ_0 – first relaxation time, s
$\boldsymbol{\phi}$ – microrotation vector
$\boldsymbol{\phi}_2$ – microrotation component
ψ – change in volume fraction field

1 Introduction

The generalized thermoelasticity theories have been developed with the goal of removing the paradox of infinite speed of heat propagation inherent in the classical coupled dynamical thermoelasticity theory discussed by Biot [1]. In the generalized theories of thermoelasticity, the governing equations involve thermal relaxation times and they are of hyperbolic type. The extended thermoelasticity theory by Lord and Shulman introduces one relaxation time in the thermoelastic process and the temperature-rate-dependent theory of thermoelasticity by Green and Lindsay, which takes into account two relaxation times, are two well established generalized theories of thermoelasticity [2, 3]. Green and Naghdi developed a generalized theory of thermoelasticity which involves thermal displacement gradient as one of the constitutive variables in contrast to the classical coupled thermoelasticity which includes temperature gradient as one of the constitutive variables [4–6].

Tzou proposed a simple-phase-lag model to treat microstructural interactions such as phonon-electron and phonon scattering via two phase-lags; the first is the phase lag phase of temperature gradient and the second is the phase lag phase of heat flux, to fast transient effect of thermal waves [7, 8]. Roy Choudhuri established a coupled thermoelasticity theory of three phase-lags by adding a third phase-lags of the thermal displacement gradient [9]. The general model of the equations of the formulation in the context of the three phase-lags theory is applied by many investigators.

The linear theory of micropolar elasticity is adequate to represent the behavior of such materials. For ultrasonic waves, i.e. in the case of elastic vibrations characterized by high frequencies and small wavelengths, the influence of the body microstructure becomes significant. This influence of microstructure results in the development of new types of waves, not found in the classical theory of elasticity. Metals, polymers, composites, soils, rocks, concrete is typical media with microstructures. The general theory of linear micropolar elasticity was given by Eringen [10–12]. Under this theory, solids can undergo macro-deformations and microrotations. Micropolar solids can support couple of stresses in addition to force stresses. The micropolar theory was extended to include thermal effects by Nowacki [13], Tauchert *et al.* [14], Nowacki and Olszak [15], Dhaliwal and Singh [16], Marin and Nicaise [17], Marin *et al.* [18], and Othman *et al.* [19, 20]. Among the contributions to the subject of micropolar thermoelasticity life, the works of Chandrasekharaiah [21] obtained the equa-

tions for a generalization of these equations which includes heat-flux among the constitutive variables and proved variation and reciprocal principles for such equations. Othman *et al.* [22] investigated the effect of rotation and initial stresses on generalized micropolar thermoelastic medium with a three-phase-lag. Othman and Abd-Elaziz [23] studied the effect of rotation and gravity on a micropolar magneto-thermoelastic medium with the dual-phase-lag model. Othman *et al.* [24] discussed the effect of the heat laser pulse on wave propagation of generalized thermoelastic micropolar medium with energy dissipation.

The theory of linear elastic materials with voids is one of the most important generalizations of the classical theory of elasticity. This theory has practical utility in investigating various types of geological, biological, and synthetic porous materials for which the elastic theory is inadequate. This theory is concerned with elastic materials consisting of a distribution of small pores (voids), in which the void volume is included among the kinematics variables and in the limiting case of vanishing this volume, the theory reduces to the classical theory of elasticity. Linear and nonlinear theories of voids elastic material were introduced by Cowin and Nunziato [25]. The linear theory of thermoelastic material with voids was investigated by many researchers [26–31].

The phenomenon of Thomson effect is the evolution or absorption of heat when electric current passes through a circuit composed of a single material that has a temperature difference along its length. This transfer of heat is superimposed on the common production of heat associated with the electrical resistance to currents in conductors. The Thomson effect is very important for understanding thermal power generation especially in electrical circuits and sensors. Therefore, in this paper, we want to explain the effect of thermal radiation associated with the phenomenon of the Thomson effect on a micropolar thermoelectric medium. The Thomson coefficient assumed to be a constant but the charge density of the induced electric current considered as a function of time. The impact of the Thomson effect for a homogeneous, isotropic, micropolar thermoelastic medium with voids in the context of the multi-phase-lags theory of thermoelasticity (refined multi-phase-lags theory) was investigated. The analytical expressions for the considered physical quantities were obtained by applying the normal mode analysis. Comparisons are made with the results for different values of the Thomson effect parameter and for different theories of thermoelasticity. The distributions of the considered variables are represented graphically.

2 Formulation of the problem and the basic equations

The generalized homogeneous isotropic micropolar thermoelastic medium is considered with voids. The coordinates x, y, and z is considered with origin at $y = 0$, and z-axis is setting normal to the medium. The medium is subjected to a uniform temperature T_0 in the undisturbed state. All field quantities are given in terms of the coordinates x, z, and time t. The fundamental equations for a linear, isotropic and homogeneous thermoelastic medium may be demonstrated as follows:

Displacement vector and microrotation

$$\boldsymbol{u} \equiv (u, 0, w), \qquad \boldsymbol{\phi} \equiv (0, \phi_2, 0). \tag{1}$$

Constitutive relations [10, 25]:

$$\sigma_{ij} = 2\mu\varepsilon_{ij} + k\left(u_{j,i} - \varepsilon_{ijr}\phi_r\right) + \left(\lambda e + \beta^*\psi - \upsilon\theta\right)\delta_{ij}\,, \tag{2}$$

$$m_{ij} = \alpha\phi_{r,r}\delta_{ij} + \beta\phi_{i,j} + \gamma\phi_{j,i}\,, \tag{3}$$

$$\varepsilon_{ij} = \frac{1}{2}\left(u_{i,j} + u_{j,i}\right), \tag{4}$$

where α^*, η^*, ω^*, β^*, m, ζ^* are the material constants due to presence of voids.

Equation of motion

$$\sigma_{ji,j} = \rho\ddot{u}_i\,, \tag{5}$$

where the number of overdots stand for the order of differentiation of a variable with respect to time. Using Eqs. (2) and (4), Eq. (5) can be written as

$$(\mu + k)u_{i,ii} + (\lambda + \mu)e_i + k(\varepsilon_{ijr}\phi_r)_i + \beta^*\psi_i - \upsilon\theta_i = \rho\ddot{u}_i\,. \tag{6}$$

The refined multi-phase-lags thermoelasticity theory with Thomson effect is described in [28, 32]. In this paper, the Thomson coefficient assumed to be a constant but the charge density of the induced electric current considered as a function of time:

$$K^*\left(1 + \sum_{r=1}^{N}\frac{\tau_\theta^r}{r!}\frac{\partial^r}{\partial t^r}\right)\theta_{ii} = \left(\delta + \tau_0\frac{\partial}{\partial t} + \sum_{r=1}^{N}\frac{\tau_q^{r+1}}{(r+1)!}\frac{\partial^{r+1}}{\partial t^{r+1}}\right) \times \left(\rho C_e\dot{\theta} + \upsilon T_0\dot{e} + mT_0\psi + M\rho_e^0 L_0 e\right). \tag{7}$$

Micropolar equation (see [14])

$$\varepsilon_{ijp}\sigma_{jp} + m_{ji,j} = \rho j\ddot{\phi}_i\,. \tag{8}$$

Using Eqs. (1)–(3) Eq. (8) takes the form

$$(\alpha+\beta+\gamma)\nabla(\nabla\times\phi)_i - \gamma\nabla\times(\nabla\times\phi)_i + k(\nabla\times u)_i - 2k\phi_i = \rho j\ddot{\phi}_i\,. \tag{9}$$

Voids equation

$$\alpha^*\nabla^2\psi - \eta^*\psi - \omega^*\dot{\psi} - \beta^* e + m\theta = \rho\,\zeta^*\ddot{\psi}\,. \tag{10}$$

The strain

$$e = \nabla\cdot\boldsymbol{u}. \tag{11}$$

Applying Eq. (1) into Eqs. (6) and (9), the governing equations for a micropolar thermoelastic medium with voids under the influence of Thomson effect with the refined phase-lags theory can be rewritten as:

$$(\mu+k)\nabla^2 u + (\lambda+\mu)\frac{\partial e}{\partial x} - k\frac{\partial\phi_2}{\partial z} + \beta^*\frac{\partial\psi}{\partial x} - \upsilon\frac{\partial\theta}{\partial x} = \rho\ddot{u}\,, \tag{12}$$

$$(\mu+k)\nabla^2 w + (\lambda+\mu)\frac{\partial e}{\partial z} + k\frac{\partial\phi_2}{\partial x} + \beta^*\frac{\partial\psi}{\partial z} - \upsilon\frac{\partial\theta}{\partial z} = \rho\ddot{w}\,, \tag{13}$$

$$K^*\left(1+\sum_{r=1}^{N}\frac{\tau_\theta^r}{r!}\frac{\partial^r}{\partial t^r}\right)\nabla^2\theta = \left(\delta+\tau_0\frac{\partial}{\partial t}+\sum_{r=1}^{N}\frac{\tau_q^{r+1}}{(r+1)!}\frac{\partial^{r+1}}{\partial t^{r+1}}\right)\left(\rho C_e\dot{\theta}+\upsilon T_0\dot{e}+mT_0\psi+M\rho_e^0 L_0 e\right). \tag{14}$$

$$\gamma\nabla^2\phi_2 + k\left(\frac{\partial u}{\partial z} - \frac{\partial w}{\partial x}\right) - 2k\phi_2 = \rho j\ddot{\phi}_2\,, \tag{15}$$

$$\alpha^*\nabla^2\psi - \eta^*\psi - \omega^*\dot{\psi} - \beta^* e + m\theta = \rho\,\zeta^*\ddot{\psi}\,. \tag{16}$$

Also, the stress tensor and couple stress tensor components take the form:

$$\sigma_{xx} = (2\mu+k)\frac{\partial u}{\partial x} + \lambda e + \beta^*\psi - \upsilon T, \tag{17}$$

$$\sigma_{yy} = \lambda e + \beta^*\psi - \upsilon T, \tag{18}$$

$$\sigma_{zz} = (2\mu+k)\frac{\partial w}{\partial z} + \lambda e + \beta^*\psi - \upsilon T, \tag{19}$$

$$\sigma_{xz} = \mu \frac{\partial u}{\partial z} + (\mu + k) \frac{\partial w}{\partial x} + k\phi_2 \,, \tag{20}$$

$$\sigma_{zx} = (\mu + k) \frac{\partial u}{\partial z} + \mu \frac{\partial w}{\partial x} - k\phi_2 \,, \tag{21}$$

$$m_{xy} = \gamma \frac{\partial \phi_2}{\partial x} \,, \tag{22}$$

$$m_{yx} = \beta \frac{\partial \phi_2}{\partial x} \,, \tag{23}$$

$$m_{yz} = \beta \frac{\partial \phi_2}{\partial z} \,, \tag{24}$$

$$m_{zy} = \gamma \frac{\partial \phi_2}{\partial z} \,, \tag{25}$$

$$m_{xx} = m_{yy} = m_{zz} = m_{xz} = m_{zx} = 0. \tag{26}$$

For simplifications we shall use the following non-dimensional variables:

$$\begin{gathered} \{x', z'\} = \frac{\omega}{c_1}\{x, z\}, \quad \{u', w'\} = \frac{\rho\omega c_1}{\mu}\{u, w\}, \\ \{\phi_2', \psi'\} = \frac{\rho c_1^2}{\mu}\{\phi_2, \psi\}, \quad \theta' = \frac{1}{T_0}\theta, \quad \sigma_{ij}' = \frac{\sigma_{ij}}{\mu} \,, \\ \{t', \tau_0', \tau_\theta', \tau_q'\} = \omega\{t, \tau_0, \tau_\theta, \tau_q\}, \quad m_{ij}' = \frac{\omega}{c_1 \mu} m_{ij} \cdot \upsilon \end{gathered} \tag{27}$$

where $c_1^2 = \dfrac{(\lambda + 2\mu + k)}{\rho}$ and $\omega = \dfrac{\rho C_e c_1^2}{K^*}$.

Using (27), governing Eqs. (12)–(16), become:

$$\left(\frac{\mu + k}{\rho c_1^2}\right) \nabla^2 u + \left(\frac{\lambda + \mu}{\rho c_1^2}\right) \frac{\partial e}{\partial x} - \left(\frac{k}{\rho c_1^2}\right) \frac{\partial \phi_2}{\partial z} + \left(\frac{\beta^*}{\rho c_1^2}\right) \frac{\partial \psi}{\partial x} - \upsilon \frac{\partial \theta}{\partial x} = \ddot{u}, \tag{28}$$

$$\left(\frac{\mu + k}{\rho c_1^2}\right) \nabla^2 w + \left(\frac{\lambda + \mu}{\rho c_1^2}\right) \frac{\partial e}{\partial z} + \left(\frac{k}{\rho c_1^2}\right) \frac{\partial \phi_2}{\partial x} + \left(\frac{\beta^*}{\rho c_1^2}\right) \frac{\partial \psi}{\partial z} - \upsilon \frac{\partial \theta}{\partial z} = \ddot{w}, \tag{29}$$

$$\begin{aligned} K^* \left(1 + \sum_{r=1}^{N} \frac{\tau_\theta^r}{r!} \frac{\partial^r}{\partial t^r}\right) \nabla^2 \theta = \left(\delta + \tau_0 \frac{\partial}{\partial t} + \sum_{r=1}^{N} \frac{\tau_q^{r+1}}{(r+1)!} \frac{\partial^{r+1}}{\partial t^{r+1}}\right) \\ \left(\frac{\rho C_e c_1^2}{\omega} \dot{\theta} + \frac{\upsilon^2 T_0}{\rho\omega} \dot{e} + \frac{m T_0 \upsilon}{\rho\omega^2} \psi + \frac{M \rho_e^0 L_0 \upsilon}{\rho\omega^2} e\right), \end{aligned} \tag{30}$$

$$\left[\nabla^2 - \left(\frac{\rho j c_1^2}{\gamma}\right) \frac{\partial^2}{\partial t^2} - \frac{2k c_1^2}{\gamma\omega^2}\right] \phi_2 + \frac{k c_1^2}{\gamma\omega^2} \left(\frac{\partial u}{\partial z} - \frac{\partial w}{\partial x}\right) = 0, \tag{31}$$

$$\left[\nabla^2 - \left(\frac{\rho\zeta^* c_1^2}{\alpha^*}\right)\frac{\partial^2}{\partial t^2} - \left(\frac{\omega^* c_1^2}{\alpha^*\omega}\right)\frac{\partial}{\partial t} - \frac{\eta^* c_1^2}{\alpha^*\omega^2}\right]\psi - \left(\frac{\beta^* c_1^4}{\alpha^*\omega^4}\right)e + \left(\frac{m\rho c_1^4}{\alpha^*\omega^2 v}\right)\theta = 0. \tag{32}$$

Also, the stress tensor components (17)–(21), using (27), become:

$$\sigma_{xx} = \left(\frac{2\mu + k}{\rho c_1^2}\right)\frac{\partial u}{\partial x} + \left(\frac{\lambda}{\rho c_1^2}\right)e + \left(\frac{\beta^*}{\rho c_1^2}\right)\psi - \theta, \tag{33}$$

$$\sigma_{yy} = \left(\frac{\lambda}{\rho c_1^2}\right)e + \left(\frac{\beta^*}{\rho c_1^2}\right)\psi - \theta\,, \tag{34}$$

$$\sigma_{zz} = \left(\frac{2\mu + k}{\rho c_1^2}\right)\frac{\partial w}{\partial z} + \left(\frac{\lambda}{\rho c_1^2}\right)e + \left(\frac{\beta^*}{\rho c_1^2}\right)\psi - \theta, \tag{35}$$

$$\sigma_{xz} = \left(\frac{\mu}{\rho c_1^2}\right)\frac{\partial u}{\partial z} + \left(\frac{\mu + k}{\rho c_1^2}\right)\frac{\partial w}{\partial x} + \left(\frac{k}{\rho c_1^2}\right)\phi_2\,, \tag{36}$$

$$\sigma_{zx} = \left(\frac{\mu + k}{\rho c_1^2}\right)\frac{\partial u}{\partial z} + \left(\frac{\mu}{\rho c_1^2}\right)\frac{\partial w}{\partial x} - \left(\frac{k}{\rho c_1^2}\right)\phi_2\,. \tag{37}$$

Similarly, the couple stress tensor components (22)–(25), using (27), take the form:

$$m_{xy} = \left(\frac{\gamma\omega^2}{\rho c_1^4}\right)\frac{\partial \phi_2}{\partial x}\,, \tag{38}$$

$$m_{zy} = \left(\frac{\gamma\omega^2}{\rho c_1^4}\right)\frac{\partial \phi_2}{\partial z}\,, \tag{39}$$

$$m_{yx} = \left(\frac{\beta\omega^2}{\rho c_1^4}\right)\frac{\partial \phi_2}{\partial x}\,, \tag{40}$$

$$m_{yz} = \left(\frac{\beta\omega^2}{\rho c_1^4}\right)\frac{\partial \phi_2}{\partial z}\,. \tag{41}$$

We introduce the displacement potentials $q_1(x, z, t)$ and $q_2(x, z, t)$ which are related to displacement components, and in effect we obtain:

$$\begin{aligned} u &= \frac{\partial q_1}{\partial x} + \frac{\partial q_2}{\partial z}\,, & w &= \frac{\partial q_1}{\partial z} - \frac{\partial q_2}{\partial x}\,, \\ e &= \frac{\partial u}{\partial x} + \frac{\partial w}{\partial z} = \nabla^2 q_1\,, & \frac{\partial u}{\partial z} - \frac{\partial w}{\partial x} &= \nabla^2 q_2\,. \end{aligned} \tag{42}$$

Using (42), Eqs. (28)–(32) become:

$$\left(\nabla^2 - \frac{\partial^2}{\partial t^2}\right) q_1 + \left(\frac{\beta^*}{\rho c_1^2}\right) \psi - \theta = 0, \tag{43}$$

$$\left[\left(\frac{\mu + k}{\rho c_1^2}\right) \nabla^2 - \frac{\partial^2}{\partial t^2}\right] q_2 - \left(\frac{k}{\rho c_1^2}\right) \phi_2 = 0, \tag{44}$$

$$K \left(1 + \sum_{r=1}^{N} \frac{\tau_\theta^r}{r!} \frac{\partial^r}{\partial t^r}\right) \nabla^2 \theta = \left(\delta + \tau_0 \frac{\partial}{\partial t} + \sum_{r=1}^{N} \frac{\tau_q^{r+1}}{(r+1)!} \frac{\partial^{r+1}}{\partial t^{r+1}}\right) \left(\frac{\rho C_e c_1^2}{\omega} \dot{\theta} + \frac{\upsilon^2 T_0}{\rho \omega} \nabla^2 \dot{q}_1 + \frac{m T_0 \upsilon}{\rho \omega^2} \psi + \frac{M \rho_e^0 L_0 \upsilon}{\rho \omega^2} \nabla^2 q_1\right), \tag{45}$$

$$\left[\nabla^2 - \left(\frac{\rho j c_1^2}{\gamma}\right) \frac{\partial^2}{\partial t^2} - 2 \frac{k c_1^2}{\gamma \omega^2}\right] \phi_2 + \frac{k c_1^2}{\gamma \omega^2} \nabla^2 q_2 = 0, \tag{46}$$

$$\left[\nabla^2 - \frac{\rho \zeta^* c_1^2}{\alpha^*} \frac{\partial^2}{\partial t^2} - \frac{\omega^* c_1^2}{\alpha^* \omega} \frac{\partial}{\partial t} - \frac{\eta^* c_1^2}{\alpha^* \omega^2}\right] \psi - \left(\frac{\beta^* c_1^4}{\alpha^* \omega^4}\right) \nabla^2 q_1 + \left(\frac{m \rho c_1^4}{\alpha^* \omega^2 \upsilon}\right) \theta = 0. \tag{47}$$

3 Normal mode analysis

The solution of the considered physical variable can be decomposed in terms of normal modes as the following from:

$$[u, w, q_1, q_2, T, \phi_2, \psi, \sigma_{ij}](x, z, t) = [u^*, w^*, q_1^*, q_2^*, T^*, \phi_2^*, \psi^*, \sigma_{ij}^*](z) e^{(st + iax)}, \tag{48}$$

where the complex time constant is s, a is the wave number in the x-direction, and i represent the imaginary unit.

Using Eq. (48), Eqs. (43)–(47) take the form:

$$[D^2 - a_1] q_1^* + a_2 \psi^* - \theta^* = 0, \tag{49}$$

$$[a_3 D^2 - a_4] q_2^* - a_5 \phi_2^* = 0, \tag{50}$$

$$[D^2 - a_6] \phi_2^* + a_7 [D^2 - a^2] q_2^* = 0, \tag{51}$$

$$[D^2 - a_8] \psi^* - a_9 [D^2 - a^2] q_1^* + a_{10} \theta^* = 0, \tag{52}$$

$$[a_{11} D^2 - a_{12}] \theta^* - a_{13} [D^2 - a^2] q_1^* - a_{14} \psi^* = 0. \tag{53}$$

Eliminating q_1^*, ψ^*, and θ^* between Eqs. (49), (52), and (53), we obtain

$$[D^6 - A_1 D^4 + A_2 D^2 - A_3]\{q_1^*, \psi^*, \theta^*\} = 0. \tag{54}$$

Equation (54) can be factorized as

$$(D^2 - k_1^2)(D^2 - k_2^2)(D^2 - k_3^2)\{q_1^*, \theta^*, \psi^*\} = 0, \tag{55}$$

where $k_n^2 (n = 1, 2, 3)$ are the roots of the characteristic equation of (54), and

$$D = \frac{\mathrm{d}}{\mathrm{d}z}, \quad a_1 = a^2 + s^2, \quad a_2 = \frac{\beta^*}{\rho c_1^2}, \quad a_0 = \frac{\delta\omega^*}{c_1^2}, \quad a_3 = \frac{\mu + k}{\rho c_1^2},$$

$$a_4 = a_3 a^2 + s^2, \quad a_5 = \frac{k}{\rho c_1^2}, \quad a_6 = a^2 + \frac{\rho j s^2 c_1^2}{\gamma} + \frac{2k c_1^2}{\gamma\omega^2}, \quad a_7 = \frac{k c_1^2}{\gamma\omega^2},$$

$$a_8 = a^2 + \frac{\rho\zeta^* s^2 c_1^2}{\alpha^*} + \frac{\omega^* s c_1^2}{\alpha^*\omega} + \frac{\eta^* c_1^2}{\alpha^*\omega^2}, \quad a_9 = \frac{\beta^* c_1^4}{\alpha^*\omega^4}, \quad a_{10} = \frac{m\rho a_0 c_1^4}{\alpha^*\omega^2 \upsilon},$$

$$a_{11} = K^* \left(1 + \sum_{r=1}^{N} \frac{\tau_\theta^r}{r!} s^r\right), \quad a_0 = \delta + \tau_0 s + \sum_{r=1}^{N} \frac{\tau_q^{r+1}}{(r+1)!} s^{r+1},$$

$$r_0 = \frac{\rho C_e C_1^2 s^2}{\omega},$$

$$a_{12} = a_{11} a^2 + r_0 a_0, \quad a_{13} = \frac{\upsilon^2 T_0 s a_0}{\rho\omega} + \frac{M\rho_e^0 L_0 \upsilon a_0}{\rho\omega^2}, \quad a_{14} = \frac{m T_0 a_0}{\rho\omega^2},$$

$$A_0 = \frac{1}{a_{11}}, \quad A_1 = A_0\left(-a_9 a_2 a_{11} + a_{12} + a_{13} + a_1 a_{11} + a_8 a_{11}\right),$$

$$A_2 = A_0\Big(a_8 a_{12} - a_9 a^2 a_2 a_{11} + a_1 a_8 a_{11} + a_{10} a_{14} - a_9 a_2 a_{12}$$
$$- a_9 a_{14} + a_{13} a_8 + a_1 a_{12} - a_{13} a_2 a_{10} + a_{13} a^2\Big),$$

$$A_3 = A_0\Big(a_1 a_8 a_{12} - a_9 a^2 a_2 a_{12} - a_9 a^2 a_{14} + a_1 a_{10} a_{14}$$
$$- a_{13} a^2 a_2 a_{10} + a_{13} a^2 a_8\Big).$$

The solution of Eq. (55) bounds at $z \to \infty$, are given by

$$(q_1^*, \psi^*, \theta^*)(z) = \sum_{n=1}^{3} (1, H_{1n}, H_{3n}) M_n e^{-k_n z}. \tag{56}$$

In the same manner, eliminating q_2^* and ϕ_2^*, between Eqs. (50) and (51), we get

$$[D^4 - B_1 D^2 + B_2]\{q_2^*, \phi_2^*\} = 0. \tag{57}$$

Solution of of the characteristic equation of Eq. (57), bound at $z \to \infty$, are given by

$$(q_2^*, \phi_2^*)(z) = \sum_{h=4}^{5} (1, R_{1h}) M_h e^{-k_h z}, \tag{58}$$

where k_h^2 $(h = 4, 5)$ are the roots of the characteristic equation of Eq. (57), and

$$\begin{aligned}
B_0 &= \frac{1}{a_3}, & B_1 &= B_0(a_4 + a_3 a_6 - a_5 a_7), \\
B_2 &= B_0(a_4 a_6 - a_5 a_7 a^2), & n &= 1, 2, 3, \\
H_{1n} &= \frac{a_9(k_n^2 - a^2) - a_{10}(k_n^2 - a_1)}{k_n^2 + a_2 a_{10} - a_8)}, & H_{2n} &= k_n^2 - a_1 + a_2 H_{1n}, \\
R_{1h} &= \frac{a_3 k_h^2 - a_4}{a_5}, & h &= 4, 5.
\end{aligned}$$

In order to obtain the displacement components u^*, w^* using Eqs. (56), (58) into Eq. (42), respectively, we get:

$$u^*(z) = \sum_{n=1}^{3} ia M_n e^{-k_n z} - \sum_{h=4}^{5} k_h M_h e^{-k_h z}, \tag{59}$$

$$w^*(z) = -\sum_{n=1}^{3} k_n M_n e^{-k_n z} - \sum_{h=4}^{5} ia R_{1h} M_h e^{-k_h z}. \tag{60}$$

The strain is

$$e^*(z) = \sum_{n=1}^{3} H_{3n} M_n e^{-k_n z}. \tag{61}$$

Introducing the above equations into Eqs. (33)–(41), yields:

$$\sigma_{xx}^*(z) = \sum_{n=1}^{3} H_{4n} M_n e^{-k_n z} - \sum_{h=4}^{5} R_{2h} M_h e^{-k_h z}, \tag{62}$$

$$\sigma_{yy}^*(z) = \sum_{n=1}^{3} H_{5n} M_n e^{-k_n z}, \tag{63}$$

$$\sigma_{zz}^*(z) = \sum_{n=1}^{3} H_{6n} M_n e^{-k_n z} + \sum_{h=4}^{5} R_{2h} M_h e^{-k_h z}, \tag{64}$$

$$\sigma^*_{xz}(z) = \sum_{n=1}^{3} H_{7n} M_n e^{-k_n z} + \sum_{h=4}^{5} R_{3h} M_h e^{-k_h z}\,, \tag{65}$$

$$\sigma^*_{zx}(z) = \sum_{n=1}^{3} H_{7n} M_n e^{-k_n z} + \sum_{h=4}^{5} R_{4h} M_h e^{-k_h z}\,, \tag{66}$$

$$(m^*_{xy}, m^*_{zy}, m^*_{yx}, m^*_{yz})(z) = \sum_{h=4}^{5} (R_{5h}, R_{6h}, R_{7h}, R_{8h}) M_h e^{-k_h z}\,, \tag{67}$$

where M_n $(n = 1, 2, 3, 4, 5)$ are some constants and

$$r_7 = \frac{2\mu + k}{\rho c_1^2}\,, \quad r_8 = \frac{\lambda}{\rho c_1^2}\,, \quad r_9 = \frac{\beta^*}{\rho c_1^2}\,, \quad r_{10} = \frac{\mu}{\rho c_1^2}\,,$$
$$r_{11} = \frac{\mu + k}{\rho c_1^2}\,, \quad r_{12} = \frac{k}{\rho c_1^2}\,, \quad r_{13} = \frac{\gamma\omega^2}{\rho c_1^4}, \quad r_{14} = \frac{\beta\omega^2}{\rho c_1^4}\,,$$
$$H_{3n} = k_n^2 - a^2, \quad R_{2h} = iar_7 k_h\,,$$
$$H_{4n} = r_8(k_n^2 - a^2) - a^2 r_7 + r_9 H_{1n} - H_{2n}\,,$$
$$R_{3h} = r_{10}k_h^2 + r_{11}R_{1h}a^2 + r_{12}R_{1h}\,, \quad H_{7n} = -ia(r_{10} + r_{11})k_n\,,$$
$$R_{4h} = r_{11}k_h^2 + (r_{10}a^2 - r_{12})R_{1h}\,, \quad R_{5h} = iar_{13}R_{1h}\,, \quad R_{8h} = -k_h r_{14} R_{1h}\,,$$
$$R_{7h} = iar_{14}R_{1h}\,, \quad H_{5n} = r_8(k_n^2 - a^2) + r_9 H_{1n} - H_{2n}\,,$$
$$H_{6n} = r_8(k_n^2 - a^2) + k_n^2 r_7 + r_9 H_{1n} - H_{2n}\,, \quad R_{6h} = -k_h r_{13} R_{1h}\,,$$
$$n = 1, 2, 3, \quad h = 4, 5.$$

4 Boundary conditions

The determination of parameters M_1, M_2, M_3, M_4, M_5 leads to consideration of the boundary conditions at $z = 0$.

4.1 Mechanical boundary conditions

The normal stress condition (mechanically stressed by constant force F_0), and the tangential stress condition (stress free), so that

$$\sigma_{zx} = 0, \qquad \sigma_{zz} = -F_0 e^{(st+iax)}. \tag{68}$$

4.2 Condition of the couple stress

The couple stress is constant in z-direction, this implies that

$$m_{zy} = 0. \tag{69}$$

4.3 Thermal condition

The thermal shock is assumed at the surface $z = 0$, which leads to

$$\theta = \theta_0 e^{(st+iax)}, \tag{70}$$

where θ_0 is a constant temperature.

4.4 Voids condition

$$\frac{\partial \psi}{\partial z} = 0. \tag{71}$$

Using Eqs. (27) and (48) on the boundary conditions (68)–(71) and using the considered variables, we obtain:

$$H_{71}M_1 + H_{72}M_2 + H_{73}M_3 + R_{44}M_4 + R_{45}M_5 = 0, \tag{72}$$
$$H_{61}M_1 + H_{62}M_2 + H_{63}M_3 + R_{24}M_4 + R_{25}M_5 = -F_0\,, \tag{73}$$
$$R_{64}M_4 + R_{65}M_5 = 0, \tag{74}$$
$$H_{21}M_1 + H_{22}M_2 + H_{23}M_3 = \theta_0\,, \tag{75}$$
$$-k_1H_{11}M_1 - k_2H_{12}M_2 - k_3H_{13}M_3 = 0. \tag{76}$$

Using the inverse matrix method we can solve the system of algebraic Eqs. (72)–(76) and get the values of the constants M_n, $n = 1, 2, 3, 4, 5$

$$\begin{pmatrix} M_1 \\ M_2 \\ M_3 \\ M_4 \\ M_5 \end{pmatrix} = \begin{pmatrix} H_{71} & H_{72} & H_{73} & R_{44} & R_{45} \\ H_{61} & H_{62} & H_{63} & R_{24} & R_{25} \\ 0 & 0 & 0 & R_{64} & R_{65} \\ H_{21} & H_{22} & H_{23} & 0 & 0 \\ -k_1H_{11} & -k_2H_{12} & -k_3H_{13} & 0 & 0 \end{pmatrix}^{-1} \begin{pmatrix} 0 \\ -F_0 \\ 0 \\ \theta_0 \\ 0 \end{pmatrix}. \tag{77}$$

5 Particular and special cases of thermoelastic theory

We discuss some special cases for different values of the parameters considered in the problem:

(i) If we take $\tau_q = \tau_\theta = \tau_0 = 0$, $\delta = 1$,then the above analysis reduces for the coupled theory (CT).

(ii) If we take $\tau_q = \tau_\theta = 0$, $\delta = 1$, $\tau_0 > 0$, then the above analysis reduces for the Lord–Shulman (L–S) theory.

(iii) The Green–Naghdi theory of type II without energy dissipation is obtained from the above analysis when $\tau_q = \tau_\theta = 0$, $\delta = 0$, and $\tau_0 = 1$.

(iv) The simple phase-lags theory is obtained from the above analysis when $\tau_q = \tau_0 > \tau_\theta \geq 0$, $\delta = 1$, $N = 1$, and by setting the term that contains τ_q^2 equals zero.

(v) The present refined phase-lags theory is given when $\tau_q = \tau_0 > \tau_\theta \geq 0$, $\delta = 1$, and $N \geq 1$.

(vi) Neglecting Thomson effect, by taking $L_0 = 0$, in Eqs. (28)–(32) we obtain the corresponding expressions of the physical variables in micropolar thermoelasticity with voids under the effect of two temperature parameters and without the Thomson effect.

(vii) Neglecting the void effect, by neglecting the material constants due to the presence of voids, putting $(\alpha^* = \eta^* = \omega^* = \beta^* = m = \zeta^* = 0)$ in Eqs. (28)–(32).

(viii) Neglecting the micropolarity effect, by neglecting the material constants due to the presence of micropolar, putting $k = \alpha = \beta = \gamma = 0$ in Eqs. (28)–(32).

6 Numerical results and discussions

Suppose that the medium is a micropolar material available in the magnesium crystal form and being imperiled to thermal as well as mechanical

disturbances for numerical calculations. The physical constants of magnesium are adopted as Othman *et al.* [22]:

$$\mu = 4 \times 10^{10}\,\mathrm{N\,m^{-2}}, \quad \lambda = 9.4 \times 10^{10}\,\mathrm{N\,m^{-2}}, \quad \rho = 1.74 \times 10^{3}\,\mathrm{kg\,m^{-3}},$$

$$T_0 = 298\,\mathrm{K}, \quad k = 85\,\mathrm{N\,m^{-2}}, \quad K^* = 1.7 \times 10^{2}\,\mathrm{J\,m^{-1}s^{-1}deg^{-1}},$$

$$j = 2 \times 10^{-20}\,\mathrm{m^2}, \quad C_e = 1.04 \times 10^{3}\,\mathrm{kg\,m^{-3}}, \quad \rho_e^0 = 1.6 \times 10^{-19}\,\mathrm{kg\,m^{-3}},$$

$$\gamma = 0.779 \times 10^{-8}\,\mathrm{N}, \quad \beta = 2.68 \times 10^{6}\,\mathrm{N\,m^{-2}deg^{-1}},$$

$$\alpha = 1.78 \times 10^{-5}, \quad \alpha_t = 1.78 \times 10^{-5}\,\mathrm{K^{-1}}.$$

The void parameters are taken as:

$$\eta^* = 1.475 \times 10^{10}\,\mathrm{N/m^2}, \quad \alpha^* = 3.668 \times 10^{-5}\,\mathrm{N}, \quad m = 2 \times 10^{6}\,\mathrm{N/m^2 \cdot K},$$
$$\zeta^* = 1.753 \times 10^{-15}\,\mathrm{N/m^2}, \quad \omega^* = 0.0787 \times 10^{-3}\,\mathrm{N \cdot s/m^2},$$
$$\beta^* = 1.13849 \times 10^{10}\,\mathrm{N/m^2}.$$

Since we have $s = \zeta_1 + i\zeta_2$, $e^{st} = e^{\zeta_1 t}[\cos(\zeta_2 t) + i\sin(\zeta_2 t)]$ and for small values of time, thus, $\cos(\zeta_2 t) \to 1$, and $\sin(\zeta_2 t) \to 0$, therefore, $s \simeq \zeta_1$ (real) can be taken. The numerical calculations have been performed using commercial software package Matlab 7.0.4 [33]. To perform the calculations, the following values are considered; $a = 1.5$ m, $x = 0.1$ m, $\zeta_1 = 1.6$ rad/s, $\zeta_2 = -0.02$ rad/s, $M = 4$, $0 \le z \le 3$.

The following comparisons have been made in four situations:

(i) Different values of Thomson parameter L_0, ($L_0 = 0.0,\ 0.2,\ 0.3,\ 0.4$).

(ii) Different theories of thermoelasticity, namely; the refined phase-lag theory, Lord–Shulman theory, Green–Naghdi theory of type II, and a coupled theory.

(iii) Effect of thermal condition, different values of temperature applied θ_0, ($\theta_0 = 0.10, 0.13, 0.16$).

(iv) Effect of mechanical condition, different values of applied force F_0, ($F_0 = 0.10, 0.11, 0.12$).

Figures 1–10 give a comparison of the results obtained for the displacement components, strain, temperature, stress components, microrotation component, change in the volume fraction field, and the couple stress tensor components, against the z-direction for different values of the Thomson effect

parameter $L_0 = 0.0$, 0.2, 0.3 and 0.4. We can note that the Thomson effect parameter has significant effects on all the studied fields. Figures 1, 2, 3, and 4 show that the distributions of the displacement components, u, w, the strain, e, and the temperature θ, decrease with the increase in the value of L_0.

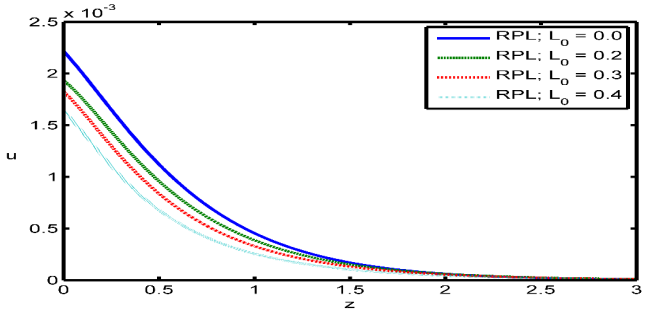

Figure 1: Distribution of the displacement component u versus z.

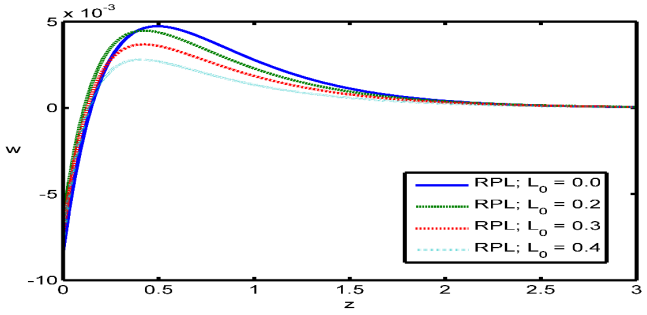

Figure 2: Distribution of the displacement component w versus z.

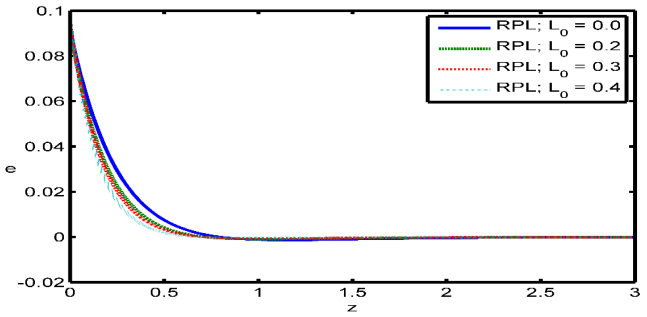

Figure 3: Distribution of the strain e versus z.

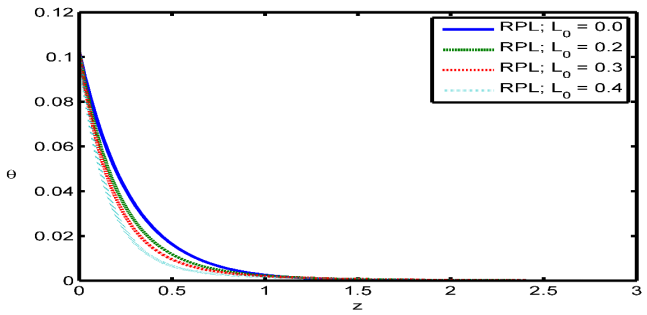

Figure 4: Distribution of the temperature θ versus z.

Figures 5 and 6 show that the Thomson effect parameter has large effects on the values of the stress components, σ_{zz} and σ_{zx}.

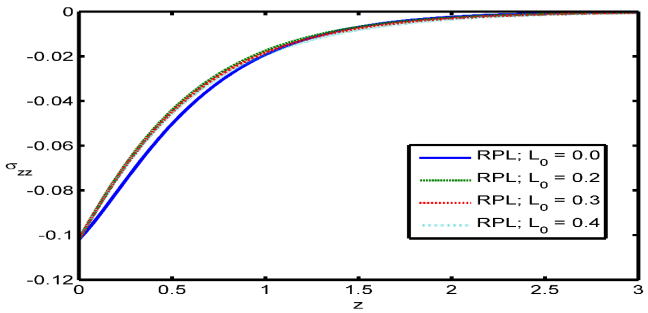

Figure 5: Distribution of the stress component σ_{zz} versus z.

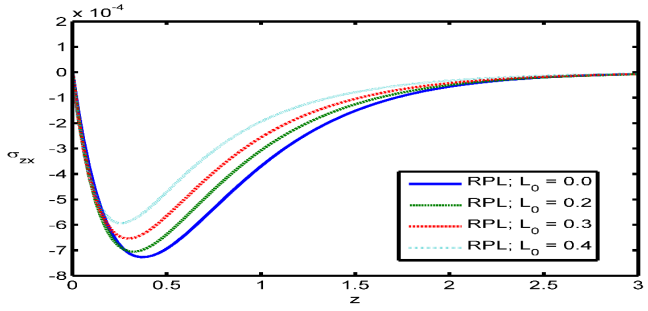

Figure 6: Distribution of the stress component σ_{zx}versus z.

Figures 7, 8, and 9 depict the distribution of the microrotation component, the change in the volume fraction field, and the couple stress tensor

component, against the distance, z. It is observed that the values of ϕ_2, ψ and m_{yx} decrease with the increase in the value of the Thomson effect parameter, L_0.

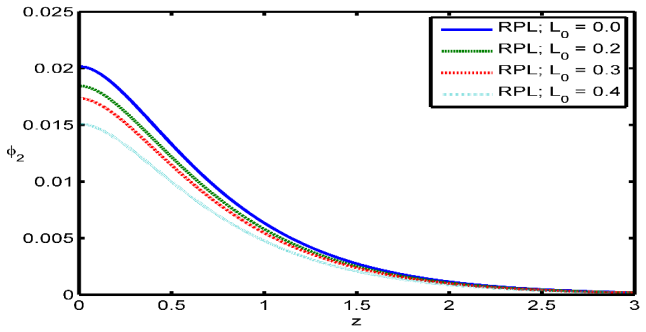

Figure 7: Distribution of the stress component σ_{zz} versus z.

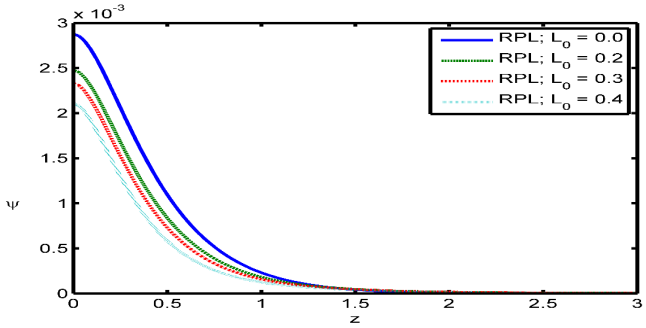

Figure 8: Distribution of the change in the volume fraction field ψ versus z.

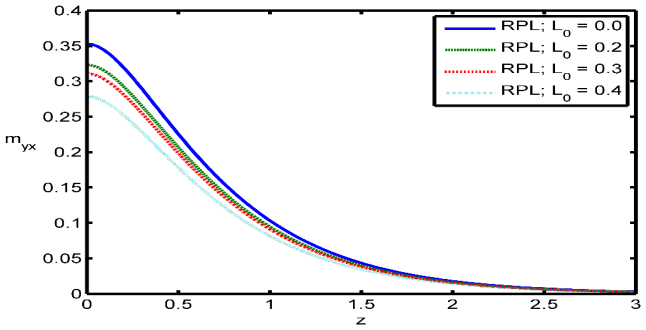

Figure 9: Distribution of the couple stress tensor component m_{yx} versus z.

Figure 10 shows the variation of the couple stress tensor component m_{zy} against the distance z. It can be seen that; the couple stress tensor component m_{zy} starts from a zero value, which satisfies the boundary conditions.

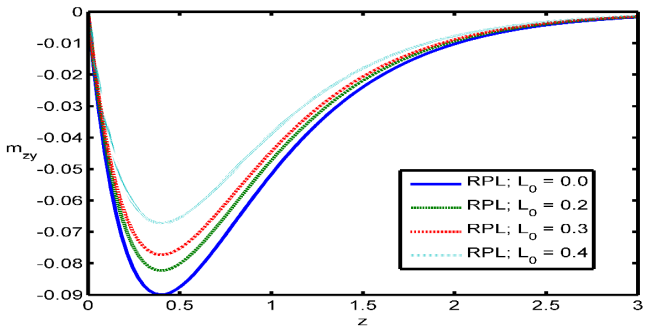

Figure 10: Distribution of the couple stress tensor component m_{zy} versus z.

Figures 11–20 show the variations of some physical variables at Thomson effect parameter $L_0 = 0.2$ for different theories of thermoelasticity, namely: the refined phase-lags theory, the Green–Naghdi theory of type II, the Lord–Shulman theory and the coupled theory. Figure 11 shows that the relative difference between theorems for the displacement component u. It can be seen that along the z-direction, the refined phase-lags theory gives the smallest value of u, while the coupled theory yields the highest ones.

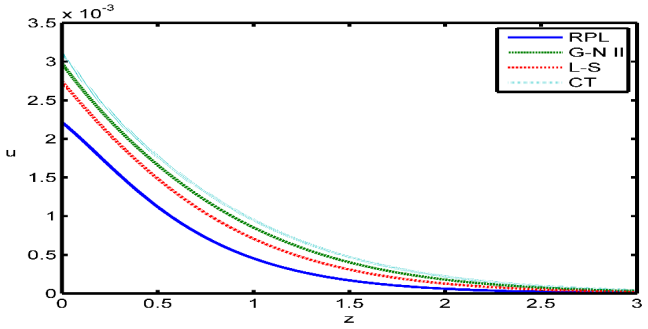

Figure 11: Distribution of the displacement component u versus z.

Figure 12 shows that the displacement component u, increases as z increases for $0 \leq z \leq 0.6$ and decreases for $0.6 \leq z \leq 2.7$, while the values are the same for $z \geq 2.7$. Figures 13 and 14 depict the variations of the strain, e, and temperature, θ, against the distance z. It can be observed that along

the z-direction, the refined phase-lags theory gives the smallest value of e and θ while the coupled theory yields the highest values. Figure 15 shows the variation of the stress component σ_{zz} against the distance z. For all theories, the values of σ_{zz} increase as z increases.

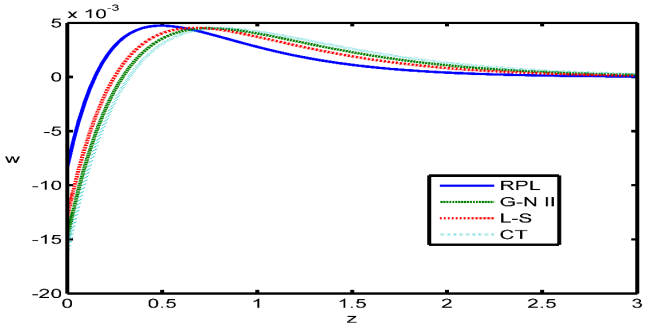

Figure 12: Distribution of the displacement component w versus z.

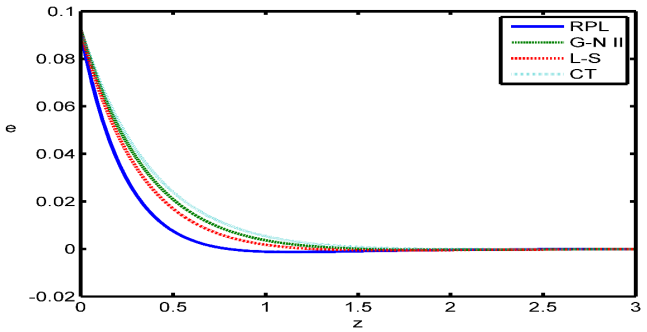

Figure 13: Distribution of the strain e versus z.

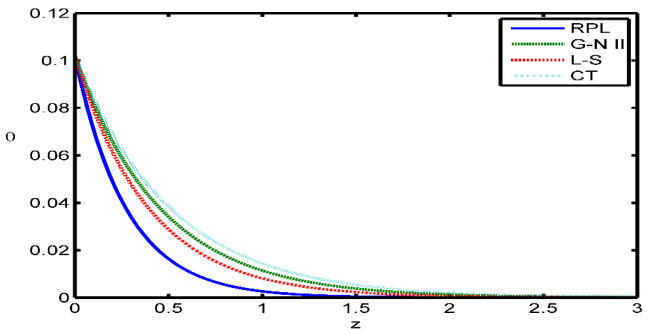

Figure 14: Distribution of the temperature θ versus z.

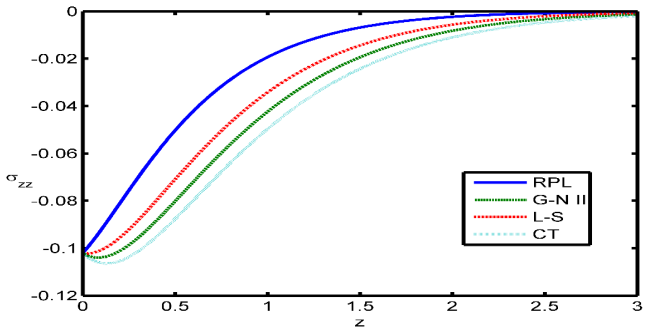

Figure 15: Distribution of the stress component σ_{zz} versus z.

Figure 16 shows that the stress component σ_{zx} decreases as distance z increases in the range $0 \leq z \leq 0.6$ increases in the range $0.6 \leq z \leq 3$ while the values are the same for $z \geq 3$.

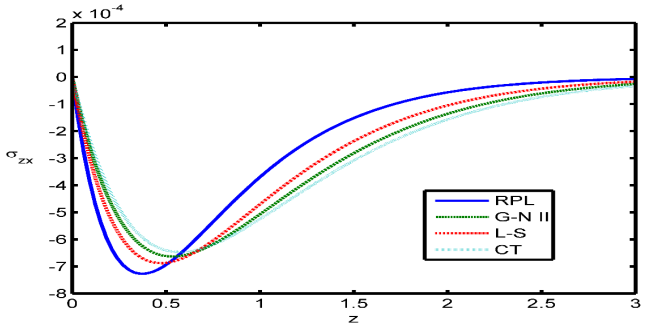

Figure 16: Distribution of the stress component σ_{zx} versus z.

Figures 17, 18, and 19 depict that the distribution of the microrotation component, the change in the volume fraction field, and the couple stress tensor component against the distance z. It is observed that: along the z-direction, the refined phase-lags theory gives the smallest value of ϕ_2, ψ and m_{yx}, while the coupled theory yields the highest ones.

Figure 20 illustrates the variation of the couple stress tensor component m_{zy} against the distance z. It can be seen that; along the $z-$direction, the coupled theory gives the smallest value of m_{zy}, while the refined phase-lags theory yields the highest value.

Figures 21–27 investigate the dimensionless displacement, temperature, stress components, microrotation, change in the volume fraction field, and

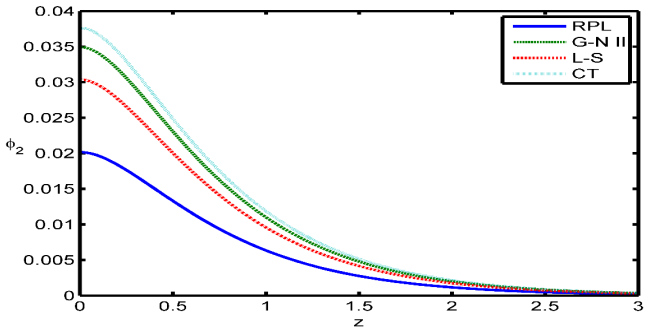

Figure 17: Distribution of the microrotation component ϕ_2 versus z.

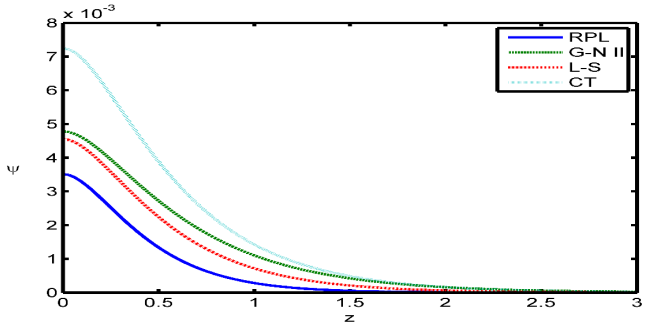

Figure 18: Distribution of the change in the volume fraction field ψ versus z.

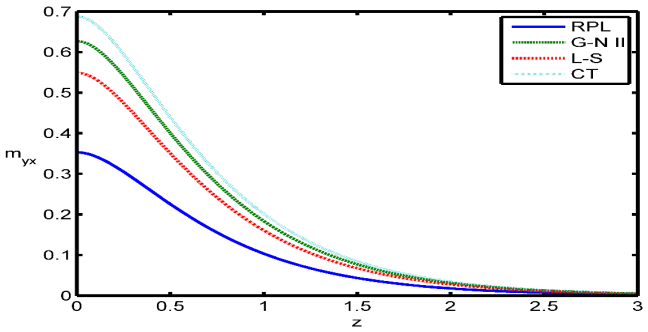

Figure 19: Distribution of the couple stress tensor component m_{yx} versus z.

couple stress tensor component with frequency of the disturbance caused by the temperature applied. In these figures, three values of temperature applied $\theta_0 = 0.1$, 0.13, and 0.16 are considered. Also, our calculations are

carried out under the impact of Thomson effect in context of refined phase lags model of thermoelasticity. In Figs. 21 and 22, the distributions of u, θ, increase when the value of θ_0 increases with clears difference. In Figs. 23

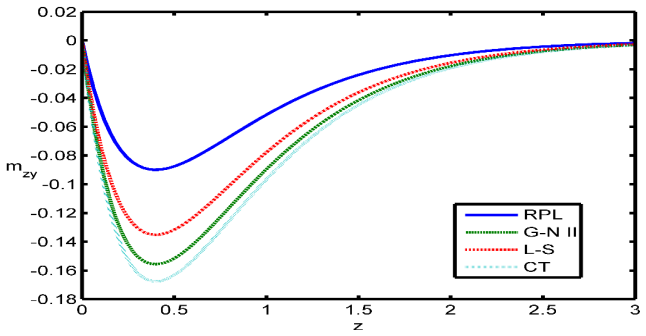

Figure 20: Distribution of the couple stress tensor component m_{zy} versus z.

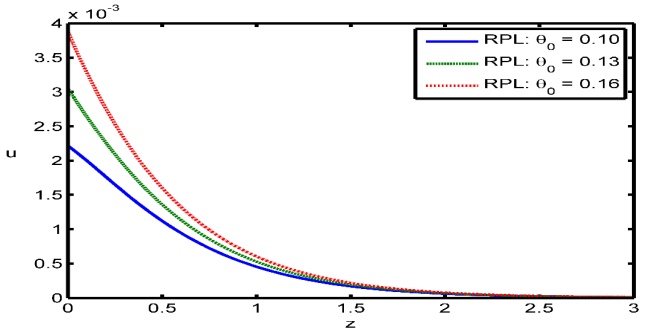

Figure 21: Distribution of the displacement component u versus z.

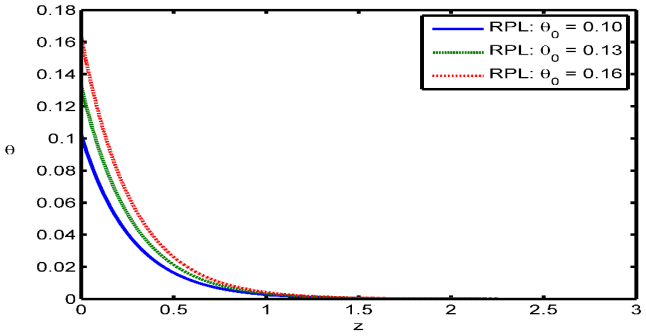

Figure 22: Distribution of the temperature θ versus z.

and 24, the distributions of stress σ_{zz}, σ_{zx}, decrease when the value of θ_0 increases. Figures 25–27, show the temperature applied, θ_0, has an important effect on the distributions of ϕ_2, ψ, and m_{zy}.

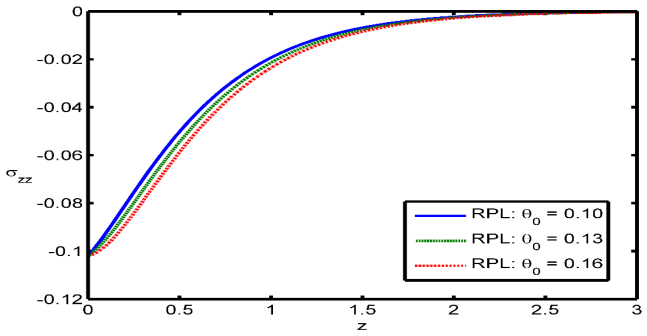

Figure 23: Distribution of the stress component σ_{zz} versus z.

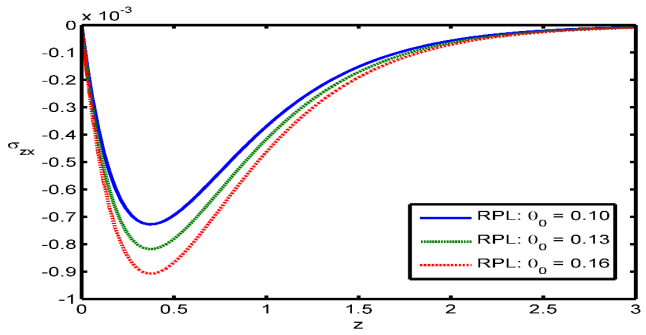

Figure 24: Distribution of the stress component σ_{zx} versus z.

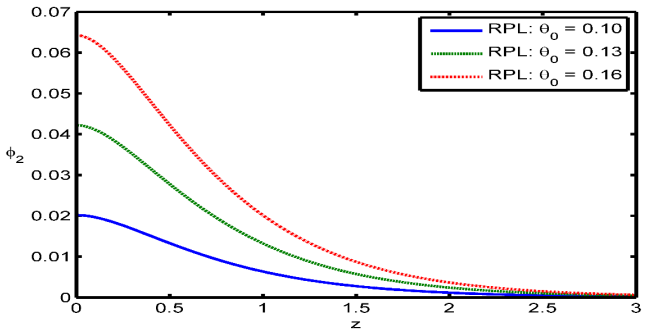

Figure 25: Distribution of the microrotation component ϕ_2 versus z.

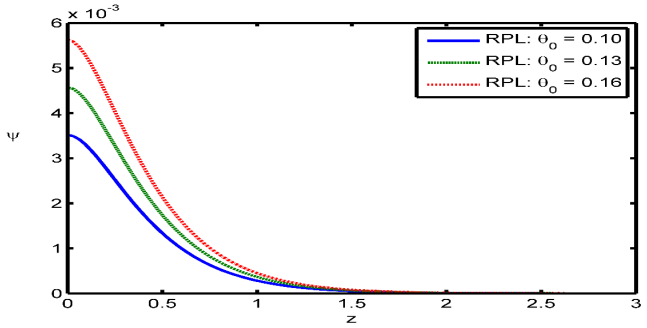

Figure 26: Distribution of the change in the volume fraction field ψ versus z.

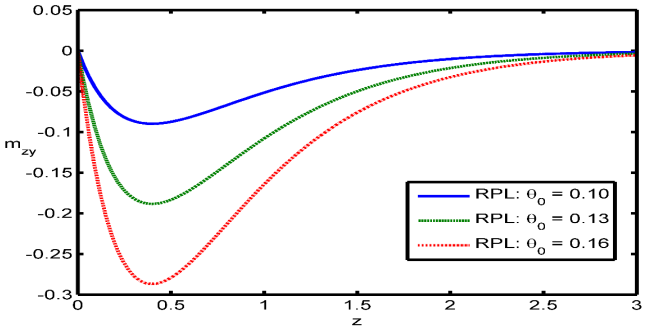

Figure 27: Distribution of the couple stress tensor component m_{zy} versus z.

Figures 28–32 show the variations of w, σ_{zz}, σ_{zx}, ϕ_2 and m_{zy} versus z, due to concentrated force, F_0. In these figures, we assumed three values for force as $F_0 = 0.1$, 0.11, and 0.12. Figure 28 shows that the distribution of

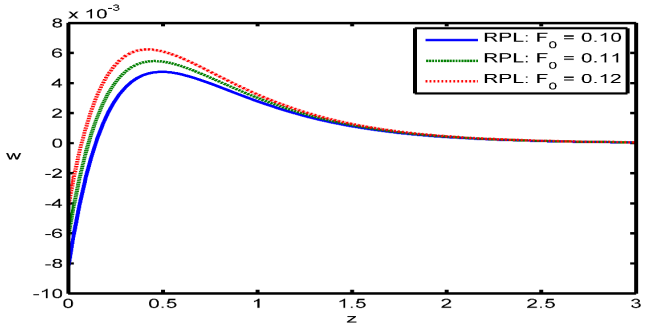

Figure 28: Distribution of the displacement component w versus z.

the displacement component w increases with the increase in the value of the force F_0. Figures 29–31 depict the variations of stresses σ_{zz}, σ_{zx}, and microrotation, ϕ_2, against the distance z. It can be observed that; the parameter F_0, has a decreasing effect on the distributions of these quantities.

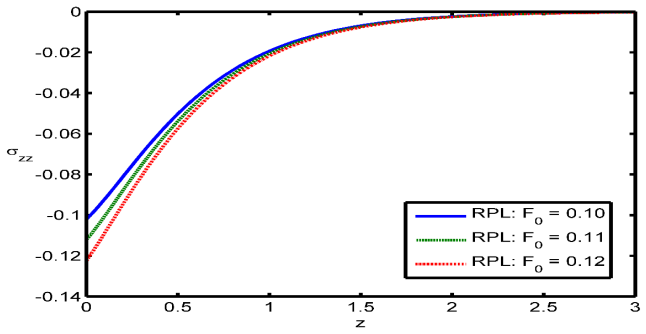

Figure 29: Distribution of the stress component σ_{zz} versus z.

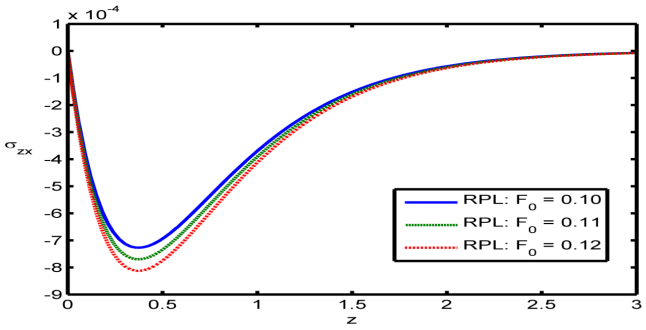

Figure 30: Distribution of the stress component σ_{zx} versus z.

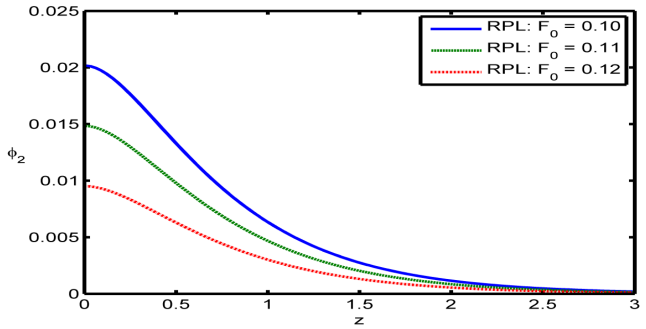

Figure 31: Distribution of the microrotation component ϕ_2 versus z.

Figure 32 represents the couple stress tensor m_{xy} calculated for different z values with applied force as the parameter. It is found that the distribution of m_{xy} increases when the value of F_0, increases.

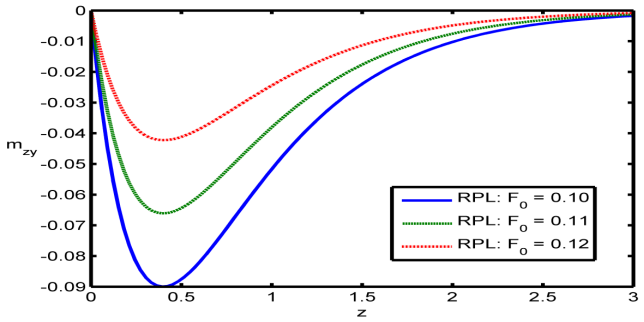

Figure 32: Distribution of the couple stress tensor component m_{zy} versus z.

Figures 33–37 represent the application of the refined phase-lags theory to obtain three-dimensional surface curves for the physical quantities of dis-

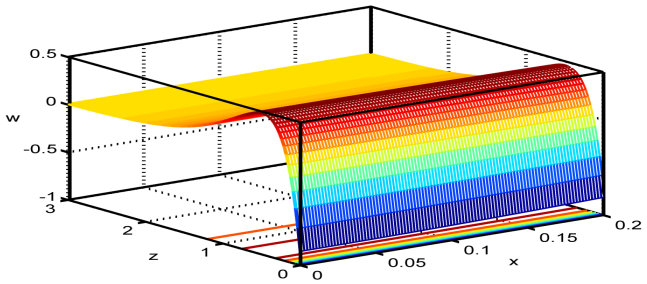

Figure 33: Three-dimensional curve distribution of the displacement component w versus distance.

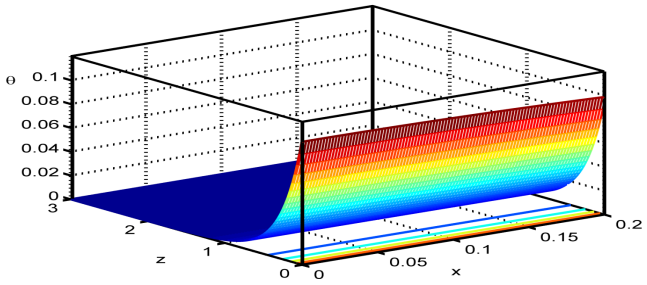

Figure 34: Three-dimensional curve distribution of the thermodynamic temperature θ versus distance.

placement component, temperature, stress component, microrotation, and couple stress tensor for the Thomson effect parameter on a thermoelastic micropolar medium consisting of voids. Whenever the vertical component of distance is part of the discussion to evaluate the dependency of physical variables on them, these figures may turn out to be extremely useful.

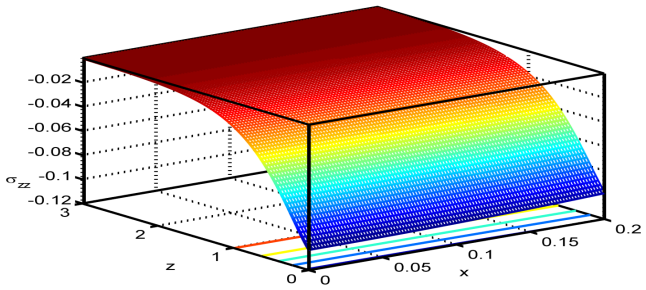

Figure 35: Three-dimensional curve distribution of the stress component σ_{zz} versus distance.

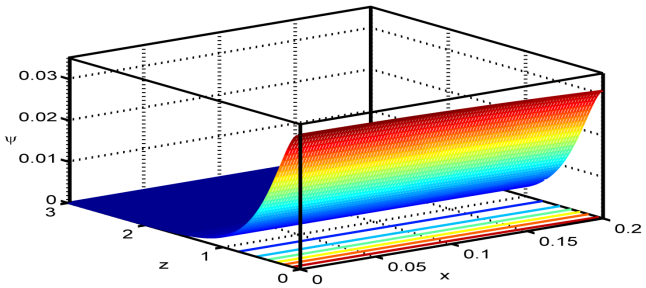

Figure 36: Three-dimensional curve distribution of the change in the volume fraction field ψ versus distance.

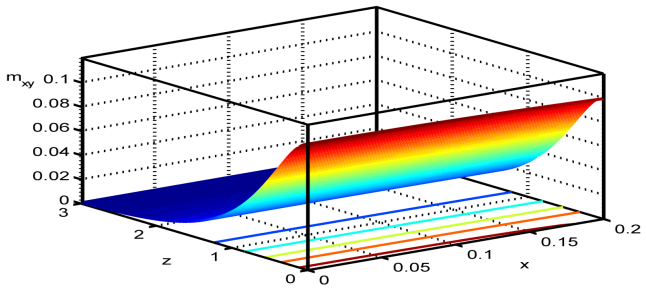

Figure 37: Three-dimensional curve distribution of the couple stress tensor component m_{xy} versus distance.

7 Conclusions

A refined multi-phase-lags micropolar thermoelasticity theory for a homogeneous medium with voids under the influence of Thomson effect has been investigated. The results concluded from the above analysis can be summarized as follows. The Thomson effect parameter has an observable effect on the distribution of the physical quantities as shown in the previous analytical solution and discussion. The physical quantities are satisfying all the boundary conditions. The used method is applicable to a wide range of thermodynamics and thermoelasticity problems. The value of all physical quantities converges to zero with an increase in distance z and all functions are continuous.

Acknowledgements The authors thank Taif University Researchers Supporting Project Number (TURSP-2020/230), Taif University, Taif, Saudi Arabia.

Received 2 March 2021

References

[1] Biot M.A.: *Thermoelasticity and irreversible thermodynamics*. J. Appl. Phys. **7**(1956), 3, 240–253.

[2] Lord H.W., Shulman Y.: *A generalized dynamical theory of thermoelasticity*. J. Mech. Phys. Sol. **15**(1967), 5, 299–309.

[3] Green A.E., Lindsay K.A.: *Thermoelasticity*. J. Elast. **2**(1972), 1, 1–7.

[4] Green A.E., Naghdi P.M.: *A re-examination of the basic postulates of thermomechanics*. Proc. R. Soc. Lond. A **432**(1991), 1885, 171–194.

[5] Green A.E., Naghdi P.M.: *On undamped heat wave in elastic solids*. J. Therm. Stress. **15**(1992), 2, 253–264.

[6] Green A.E., Naghdi P.M.: *Thermoelasticity without energy dissipation*. J. Elast. **31**(1993), 189–209.

[7] Tzou D.Y.: *The generalized lagging response in small-scale and high-rate heating*. Int. J. Heat Mass Trans. **38**(1995), 17, 3231–3240.

[8] Tzou D.Y.: *A unified field approach for heat conduction from macro- to micro-scales*. J. Heat Trans. **117**(1995), 1, 8–16.

[9] Roy Choudhuri S.K.: *On a thermoelastic three-phase-lag model*. J. Therm. Stress. **30**(2007), 3, 231–238.

[10] Eringen A.C.: *Linear theory of micropolar elasticity*. ONR Techn. Rep. **29** (School of Aeronautics, Aeronautics and Engineering Science), Purdue Univ., West Lafayett 1965.

[11] Eringen A.C.: *A unified theory of thermomechanical materials*. Int. J. Eng. Sci. **4**(1966), 2, 179–202.

[12] Eringen A.C.: *Linear theory of micropolar elasticity*. J. Math. Mech. **15**(1966), 6, 909–924.

[13] Nowacki W.: *Couple stresses in the theory of thermoelasticity III*. Bull. Acad. Pol. Sci. Tech. Ser. Sci. Tech. **14**(1966), 8, 801–809.

[14] Tauchert T.R., Claus Jr. W.D., Ariman T.: *The linear theory of micropolar thermo- elasticity*. Int. J. Eng. Sci. **6**(1968), 1, 36–47.

[15] Nowacki W., Olszak W. (Eds.): *Micropolar Thermoelasticity*. CISM Courses and Lectures 151, Springer-Verlag, Vienna 1974.

[16] Dhaliwal R.S., Singh A.: *Micropolar thermoelasticity*. In: Thermal Stresses II (R.B. Hetnarski, Ed.), Elsevier, Amsterdam 1987.

[17] Marin M., Nicaise S.: *Existence and stability results for thermoelastic dipolar bodies with double porosity*. Continuum Mech. Thermodyn. **28**(2016), 6, 1645–1657.

[18] Marin M., Ellahi R., Chirilă A.: *On solutions of Saint–Venant'S problem for elastic dipolar bodies with voids*. Carpathian J. Math. **33**(2017), 2, 219–232.

[19] Othman M.I.A., Hasona W.M., Abed-Elaziz E.M.: *Effect of rotation on micropolar generalized thermoelasticity with two temperatures using a dual-phase lag model*. Can. J. Phys. **92**(2014), 2, 148–159.

[20] Othman M.I.A., Hasona W.M., Abed-Elaziz E.M.: *The influence of thermal loading due to laser pulse on generalized micropolar thermoelastic solid with comparison of different theories*. Multi. Model. Mater. Struct. **10**(2014), 3, 328–345.

[21] Chandrasekharaiah D.S.: *Heat flux dependent micropolar thermoelasticity*. Int. J. Eng. Sci. **24**(1986), 8, 1389–1395.

[22] Othman M.I.A., Hasona W.M., Abed-Elaziz E.M.: *Effect of rotation and initial stresses on generalized micropolar thermoelastic medium with three-phase-lag*. J. Comput. Theor. Nanosci. **12**(2015), 9, 2030–2040.

[23] Othman M.I.A., Abed-Elaziz E.M.: *Effect of rotation and gravitational on a micropolar magneto-thermoelastic medium with dual-phase-lag model*. Microsyst. Tech. **23**(2017), 10, 4979–4987.

[24] Othman M.I.A., Abd-alla A.N., Abed-Elaziz E.M.: *Effect of heat laser pulse on wave propagation of generalized thermoelastic micropolar medium with energy dissipation*. Ind. J. Phys. **94**(2020), 3, 309–317.

[25] Cowin S.C., Nunziato J.W.: *Linear elastic materials with voids*. J. Elast. **13**(1983), 2, 125–147.

[26] Othman M.I.A., Abed–Elaziz E.M.: *The effect of thermal loading due to laser pulse in generalized thermoelastic medium with voids in dual-phase-lag model*. J. Therm. Stress. **38**(2015), 9, 1068–1082.

[27] Abd-Elaziz E.M., Othman M.I.A.: *Effect of Thomson and thermal loading due to laser pulse in a magneto-thermoelastic porous medium with energy dissipation*. ZAMM-Z. Angew. Math. Me. **99**(2019), 8, 201900079.

[28] Abd-Elaziz E.M., Marin M., Othman M.I.A.: *On the effect of Thomson and initial stress in a thermos-porous elastic solid under G-N electromagnetic theory.* Symmetry. **11**(2019), 3, 413–430.

[29] Othman M.I.A., Marin M.: *Effect of thermal loading due to laser pulse on thermoelastic porous media under G-N theory.* Results Phys. **7**(2017), 3863–3872.

[30] Othman M.I.A, Abd-Elaziz E.M.: *Plane waves in a magneto-thermoelastic solids with voids and microtemperatures due to hall current and rotation.* Results Phys. **7**(2017), 4253–4263.

[31] Othman M.I.A., Tantawi R.S., Eraki E.E.M.: *Effect of rotation on a semi conducting medium with two-temperature under L–S theory.* Arch. Thermodyn. **38**(2017), 2, 101–122.

[32] Chirita S., Ciarletta M., Tibullo V.: *On the thermomechanical consistency of the time differential dual-phase-lag models of heat conduction.* Int. J. Heat Mass Tran. **114**(2017), 277–285.

[33] https://matlab.mathworks.com/ (accessed 17 Feb. 2021)